

Across-horizon scattering and information transfer

V.A. Emelyanov* and F.R. Klinkhamer†

*Institute for Theoretical Physics,
Karlsruhe Institute of Technology (KIT),
76128 Karlsruhe, Germany*

Abstract

We address the question whether or not two electrically charged elementary particles can Coulomb scatter if one of these particles is inside the Schwarzschild black-hole horizon and the other outside. It can be shown that the quantum process is consistent with the local energy-momentum conservation law. This result implies that across-horizon scattering is a physical effect, relevant to astrophysical black holes. We propose a *Gedankenexperiment* which uses the quantum scattering process to transfer information from inside the black-hole horizon to outside.

Keywords: general relativity, black holes, quantum electrodynamics, Coulomb scattering

* viacheslav.emelyanov@kit.edu

† frans.klinkhamer@kit.edu

I. INTRODUCTION

Astrophysical black holes are expected to evaporate [1]. This quantum process leads to the information-loss problem in black-hole physics [2]. A final resolution of this problem could, as sometimes suggested, be based on principles that lie outside the framework of the standard semi-classical physics. But perhaps these nonstandard principles are not really needed, as the high-energy photon of quantum electrodynamics (QED) may be capable of propagating out of the black-hole horizon [3].

In this paper, we implement a particular approach to partial information recovery out of a black hole, without changing the principles of local quantum field theory. The main idea is based on the circumstance that a quantum field simultaneously exists at all spacetime points, including those of the region inside the black-hole horizon. Specifically, a quantum field is nonvanishing at each point of a given spacetime manifold and, according to the canonical (anti-)commutation relations, gives rise to random fluctuations of observables at each spacetime point, even in the vacuum state. A particle is a localized excitation, which significantly disturbs the quantum-field expectation value in its neighborhood. If the particle is sufficiently close to the black-hole horizon, the corresponding quantum-field disturbance is nonvanishing even across the black-hole horizon. Since the quantum-field disturbance is not a quantity that must propagate at a particular speed (unlike real particles), this may cause the following across-horizon effect: two charged elementary particles, located at different sides of the black-hole horizon, can scatter with each other via their quantum-field disturbances.

More concretely, the across-horizon-scattering effect can be understood as follows. In QED, the scattering interaction between charged elementary particles at tree level (virtual-photon exchange) is mathematically described by the Feynman propagator $G_F^{\mu\nu}(x, x')$ of the electromagnetic field (and, at higher orders in perturbation theory, also by the Feynman propagators of the electrically charged matter fields). This particular Green's function has a nonvanishing support for spacelike-separated points: $G_F^{\mu\nu}(x, x') \neq 0$ holds even for two spacetime points with spacelike separation, whereas, for example, the retarded Green's function $G_R^{\mu\nu}(x, x')$ vanishes identically for two spacetime points with spacelike separation. Hence, QED does not forbid the interaction between two electrically charged particles that are causally disconnected.

The crucial question, now, is if across-horizon scattering can be used to transfer information from the inside of the black-hole horizon to the outside. The present paper shows that, in practice, it may be difficult to use the across-horizon-scattering effect for information transfer but it is not impossible.

We recently became aware of an earlier calculation [4] of the emerging entanglement of two spatially separated detectors with interactions from a relativistic scalar field (see, e.g., Ref. [5] for further references). The setup of Ref. [4] is similar to ours and we will comment on it in Sec. IV.

Throughout this article, we take $c = G_N = \hbar = 1$, unless otherwise stated. Gravity is assumed to be described by standard general relativity, based on the Einstein Equivalence Principle, and the metric signature is $(+ - - -)$. Interactions of elementary particles are taken to be described by standard quantum field theory over curved spacetime.

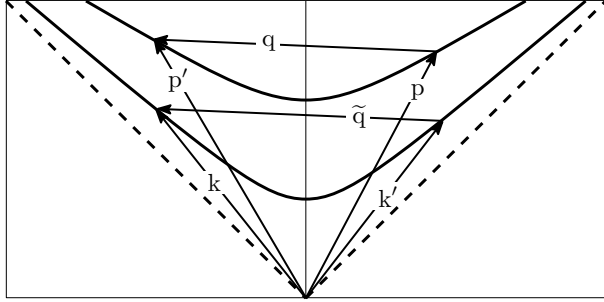


FIG. 1. Initial-particle momenta (p and k) and final-particle momenta (p' and k'), where the p and p' particles have a larger mass than the k and k' particles. Shown is a two-dimensional slice of the four-dimensional energy-momentum space, with energy along the vertical axis. The dashed line corresponds to the light-cone and all four particle momenta are timelike. Coulomb scattering (1) occurs if $q \equiv p' - p$ equals $\tilde{q} \equiv k - k'$, which corresponds to energy-momentum conservation.

II. SCATTERING

It appears that the Universe can be locally approximated by Minkowski spacetime. The Minkowski spacetime manifold is a fundamental ingredient of elementary particle physics for the description of high-energy interaction processes. In QED, the leading-order probability amplitude for the Coulomb scattering of two electrically charged elementary particles (electron e^- and muon μ^-) is represented by the following tree-level Feynman diagram [6–10]:

$$\text{out}(\mu, p'; e, k' | \mu, p; e, k)_{\text{in}} \propto \text{Feynman Diagram} \quad (1)$$

The Feynman diagram shows two incoming particles, p and k , represented by solid lines with arrows indicating flow of negative electric charge. They interact via a wavy line representing the Feynman photon propagator, with momentum q . The outgoing particles are p' and k' , represented by solid lines with arrows indicating flow of positive lepton number L_μ and negative electric charge.

with definition $q \equiv p' - p$ and arrows showing the flow of negative electric charge (and also the flow of positive lepton number, L_μ for the p and p' particles and L_e for the k and k' particles). The wavy line in the diagram on the right-hand-side of (1) stands for the Feynman photon propagator: $-ig_{\mu\nu}/(q^2 + i\epsilon)$ with a positive infinitesimal ϵ . The Feynman propagator, different from the retarded propagator, is a crucial ingredient for obtaining a unitary S -matrix (see, e.g., Sec. 3.7 and Chap. 8 of Ref. [8]). The amplitude (1) is identically zero, unless the energy-momentum conservation law is fulfilled, $p + k = p' + k'$.

In standard QED over Minkowski spacetime, the momenta of the particles before and after the Coulomb scattering are timelike four-vectors, whereas the momentum-exchange vectors $q \equiv p' - p$ and $\tilde{q} \equiv k - k'$ are spacelike four-vectors. Figure 1 gives a concrete example of these momenta, provided p' and k' satisfy the energy-momentum-conservation condition ($q = \tilde{q}$).

Next, consider a neutral and nonrotating black hole of astrophysical size (mass $M \gtrsim M_{\text{Sun}}$), so that the curvature length scale near the horizon is large compared to the Coulomb-scattering length scale to be determined shortly. In the region near the black-hole horizon, one can always introduce local Minkowski coordinates, according to the Einstein Equivalence Principle. For these local inertial coordinates (T, X, Y, Z) , part of the horizon of the black hole coincides locally with part of the light-cone shown in Fig. 2 (which is a simplified version

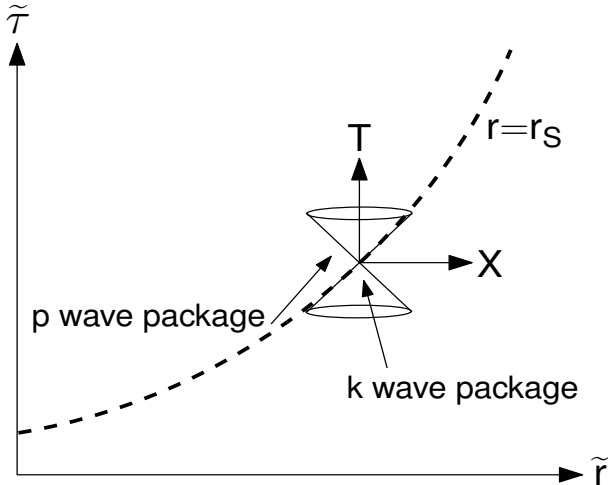


FIG. 2. In the vicinity of the black-hole horizon, coordinates can be chosen which are locally Minkowskian. A local inertial coordinate system (coordinates T , X , Y , Z) can, for instance, be embedded in the $(\tilde{\tau}, \tilde{r})$ -plane, where $\tilde{\tau}$ and \tilde{r} are, respectively, Novikov's infalling-clock time coordinate and infalling-clock comoving radial coordinate [11]. With these local inertial coordinates (Y and Z pointing out of the plane shown), the figure sketches the light-cone in the neighborhood of the Schwarzschild horizon (dashed line) at standard radial coordinate $r = r_S \equiv 2G_N M/c^2$. In addition, the trajectories of two colliding wave packages are shown, one wave package with average momentum k is positioned outside the black-hole horizon and the other wave package with average momentum p is positioned inside the horizon. These momenta k and p correspond to those of the scattering process (1) and also appear in Fig. 1. For ultrarelativistic particles, the momenta k and p are close to their respective light-cones.

of Fig. 3(a) in Ref. [11]). Locally, there is nothing in the inertial frame which marks the position of the projected horizon surface; see the second paragraph of App. A for further discussion. Remark that the black-hole metric for Novikov coordinates (as used in Fig. 2) is nonsingular at $r = R_S$; see, e.g., Sec. 31.4 in Ref. [13]. Figure 2 also shows the trajectories of two colliding wave packages, one outside the black-hole horizon with average momentum k and the other inside the horizon with average momentum p .

We are, now, ready to consider the collision of two electrically charged elementary particles of different mass, where the muon with mass m_μ is inside the black-hole horizon and the electron with mass m_e is outside. In a local inertial coordinate system (LICS) as depicted in Fig. 2, both inside-particle and outside-particle have timelike four-momenta, denoted p and k , respectively. These particles can interact with each other by “exchange of a virtual photon” if and only if the local energy-momentum conservation law is fulfilled, namely, the condition $p + k = p' + k'$ must hold (Fig. 1). In addition, the initial particles are arranged to have their closest approach (proper distance $d = d_{\min}$ at $T = T_{\min}$) near the event horizon, with the muon inside and the electron outside. Note that, strictly speaking, the minimum proper distance d_{\min} is to be determined from the initial-particle trajectories at $T \ll T_{\min}$, when interaction effects are negligible. An example of this setup is given in App. A.

The across-horizon Coulomb scattering (AHCS) with these initial momenta and trajec-

tories has a nonvanishing probability in quantum electrodynamics,

$$P_{\text{AHCS}}^{\text{LICS}} = \left(\left| \begin{array}{c} \text{Diagram of a t-channel scattering process: } p \text{ and } k \text{ are incoming particles, } p' \text{ and } k' \text{ are outgoing particles. The virtual exchange } q \text{ is shown as a wavy line.} \\ p+k=p'+k' \end{array} \right|^2 \right) r(p \text{ wave package}) \Big|_{T \leq T_{\min}} < r_S \\ r(k \text{ wave package}) \Big|_{T \leq T_{\min}} > r_S \quad (2)$$

where the standard radial coordinate r on the right-hand side is expressed in terms of the local inertial coordinates $\{T, X, Y, Z\}$ (cf. Fig. 2) and T_{\min} is the time when the separation of the initial wave packages has a minimal proper distance d_{\min} . The probability (2) will be significant if the minimal separation d_{\min} of the two initial particles is of the order of the root of the flat-spacetime cross section (with an infrared cutoff on q^2 determined by the experimental setup).

The initial particles of the scattering reaction (1) are distinguishable: the p particle has mass m_μ and lepton numbers $(L_e, L_\mu) = (0, 1)$ and the k particle has mass m_e and lepton numbers $(L_e, L_\mu) = (1, 0)$. Hence, only the t -channel diagram contributes to (2) and we get the following expression for the flat-spacetime differential cross section in the ultrarelativistic limit ($E^2 \gg m_\mu^2 \gg m_e^2$):

$$\frac{d\sigma}{d\Omega} \Big|_{\text{CM, ultrarel}}^{\text{LICS}} = \frac{\alpha^2}{2 (E_{\text{CM}})^2 (1 - \cos \theta_{\text{CM}})^2} \left[4 + (1 + \cos \theta_{\text{CM}})^2 \right], \quad (3)$$

with E_{CM} and θ_{CM} , respectively, the energy of the initial particles and the scattering angle in the center-of-mass (CM) frame. In fact, expression (3) can also be found as Eq. (5.65) in Ref. [9]. The minimal separation d_{\min} of the two initial particles in (2) must then be as close as possible to

$$d_{\text{optimal}} \sim \alpha \hbar c / E_{\text{CM}}, \quad (4)$$

where we have used the inequality $d\sigma/d\Omega \geq \alpha^2/(2E_{\text{CM}}^2)$ from (3) and have temporarily restored \hbar and c ($\alpha \approx 1/137$ is the fine-structure constant). In Fig. 4 of App. A, we have given an example of initial-particle trajectories with a finite value of the minimal separation (d_{\min}) between the initial particles. But, in principle, it is also possible to consider head-on collisions.

The result (4) for the optimal proper distance of the two colliding wave packages guarantees having a significant scattering probability, but most scattering will be in the forward direction, $\theta_{\text{CM}} \sim 0$. Thus, in the most probable case, the scattered outside-particle disappears behind the Schwarzschild horizon. Still, there is a nonvanishing probability that the outside-particle (electron) recoils due to the Coulomb interaction with the inside-particle (muon). This situation is sketched in Fig. 3 and details are given in Apps. B and C, with an example of final-particle trajectories given in Fig. 5. The ultrarelativistic recoil electron k' in Fig. 3 crosses the constant- r curves in the Penrose diagram (cf. Fig. 24(ii) in Ref. [12]) and moves away from the black-hole horizon. There is, then, a nonvanishing probability that the k' electron triggers an outside-region detector relatively near to the interaction point. This last observation is an essential ingredient of the *Gedankenexperiment* to be discussed in Sec. III.

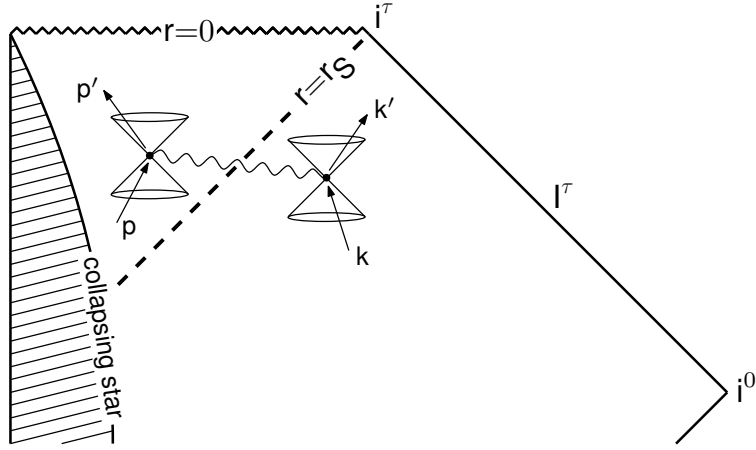


FIG. 3. Part of the Penrose conformal diagram for the Schwarzschild black hole in Kruskal–Szekeres coordinates (the full diagram is shown as Fig. 24 (ii) on p. 154 of Ref. [12], which contains further details). Also shown are two light-cones near the Schwarzschild horizon $r = r_S$ and the trajectories of two colliding wave packages, one wave package with average momentum k for the electron is positioned outside the horizon and the other wave package with average momentum p for the muon is positioned inside the horizon. These elementary particles with momenta k and p scatter by virtual-photon exchange (symbolically indicated by the wavy line) and produce, with small but nonvanishing probability, particles with momenta k' and p' . The momenta shown correspond to those of the scattering process (1). For ultrarelativistic particles, the momenta are close to their respective light-cones and there is a nonvanishing probability for significant Coulomb scattering if the k and p wave packages approach each other within a proper distance of order $\alpha \hbar c / E_{\text{CM}}$, where α is the fine-structure constant and E_{CM} the center-of-mass energy in the local inertial coordinate system.

At this moment, it may be useful to summarize the three main steps by which we arrived at this surprising result for the recoil electron:

1. According to the Einstein Equivalence Principle, the physics in a local inertial coordinate system (LICS) is the *same* as that of flat Minkowski spacetime, an example being leading-order muon-electron scattering with the Feynman propagator of the photon (Feynman propagators are needed for the correct description of the quantum theory, giving, for example, the correct value of the Lamb shift; see the discussion in, e.g., Sec. 24.1.2 of Ref. [10]).
2. The previous observation holds for a freely-falling LICS at *any* point of the Schwarzschild spacetime manifold outside the singularity, also near the horizon (part of which coincides with part of the light-cone in the LICS; cf. Fig. 2).
3. In the near-horizon LICS, muon-electron *scattering* happens for an initial muon inside the black-hole horizon and an initial electron outside the horizon, with a *nonvanishing* probability for obtaining a recoil electron in the exterior region (cf. Fig. 3 and App. C).

We now turn to an “application” of across-horizon Coulomb scattering.

III. GEDANKENEXPERIMENT

The setup of our *Gedankenexperiment* is as follows:

1. A large-mass nonrotating black hole is formed by the spherical collapse of matter and the resulting spacetime is approximately given by the static Schwarzschild metric.
2. After the black-hole formation, two experimenters, Castor and Pollux, take up their initial positions outside the Schwarzschild horizon.
3. Castor and Pollux intend to use the across-horizon scattering process from Sec. II and Fig. 3 with pre-determined initial momenta p and k (in the freely-falling frame), which are arranged to give, with largest possible probability, a nontrivial scattering event with recoil momentum k' of the outside-electron. They also intend to perform their experiments rapidly enough, so that their later inside/outside positions with respect to the Schwarzschild horizon do not change substantially.
4. Castor and Pollux, while in the exterior region, agree on the details of the procedure and get started:
 - 4a. along a fixed radial direction, Pollux stays outside the Schwarzschild horizon and Castor rapidly moves inside the horizon; once inside, Castor must act fast as his available proper time τ^C is limited, $\tau^C \leq (\pi/2) r_S/c \sim 10^{-5} \text{ s}$ (M/M_{Sun}), see, e.g., Ex. 31.4 on p. 836 in Ref. [13];
 - 4b. at a pre-arranged moment, Pollux starts to emit, at regular time intervals, appropriate electrons [each of momentum k from (1) and App. A, in the freely-falling frame] and sends out a finite number N of electrons in total ($1 \ll N < \infty$);
 - 4c. starting from the corresponding pre-arranged moment and at an appropriately adjusted rate, Castor either emits N appropriate muons [each of momentum p from (1) and App. A, in the freely-falling frame] or sends no such muons at all; in the first case, Castor writes in his message-book a “yes” and, in the second case, he writes a “no”;
 - 4d. if Castor has emitted N muons p , then Pollux’s detector (positioned at an appropriate distance away from the black-hole horizon) has a nonzero chance to register a momentum change of the exterior electron as discussed in Apps. B and C [Pollux writes “1” in his log-book if he registers a recoil electron with momentum k' and “0” if he does not register a recoil electron], but if Castor has emitted no muons p at all, then Pollux’s detector will never register a recoil electron [Pollux writes N times a “0” in his logbook];
 - 4e. after N measurements, Pollux looks at his logbook and summarizes his results as follows: a sequence of N zeros is written as “NO” and a sequence with at least a single “1” is written as “YES.”
5. According to points 4c and 4e, Castor can send a message (“yes” or “no” in his message-book), which is read by Pollux (“YES” or “NO” in his logbook).

6. As Castor's message-book is in the interior region of the Schwarzschild black-hole horizon and Pollux's log-book in the exterior region, information ("yes" or "no") has been transferred outwards, across the Schwarzschild black-hole horizon.
7. Pollux can transmit the message in his logbook ("YES" or "NO") to distant observers by classical means such as pulses of electromagnetic radiation; see Sec. IV for further discussion.

A few technical remarks are in order:

- ad 4b. Castor and Pollux's procedure can be extended by having several sequences (labeled $i = 1, \dots, I$) with each $N_i^P = N$ electrons emitted by Pollux and $N_i^C = N/0$ muons emitted by Castor, so that Castor's whole message is (yes/no, yes/no, \dots , yes/no) with I entries.
- ad 4d. As the probability for getting a measurable kick of the exterior electron is small (see Apps. B and C), N needs to be taken sufficiently large.
- ad 4e. It is, in principle, possible that Castor's N muons do not produce a recoil electron (N is large but finite) or that Pollux's detector records a false "1" (the detector may trigger even in the absence of a recoil electron), so that the read message is not error-free. Castor and Pollux may, therefore, decide to use an error-correcting code for the I -entries message mentioned in the first technical remark.

All these technical issues are engineering questions and need to be addressed. Note that the whole experimental setup of Castor and Pollux (with a muon factory, a linear accelerator for muons, an electron source, a linear accelerator for electrons, and a detector for electrons) may have a substantial mass, but still very much less than the black-hole mass M which can be made arbitrarily large (at least, in a *Gedankenexperiment*).

IV. DISCUSSION

Heuristically, across-horizon Coulomb scattering appears to be quite natural. Assume that a nonrotating astrophysical black hole is initially neutral and that, at a later moment, a particle of electric charge Q falls in radially, crossing the Schwarzschild horizon. From a macroscopic point of view, this charged particle changes the Schwarzschild black hole into a Reissner–Nordstrøm black hole of charge Q . In other words, although the charged particle was "swallowed" by the black hole, knowledge of its charge Q has not disappeared for the region outside the black-hole horizon and can still influence the outside-charges. From a microscopic point of view, this Coulomb interaction happens due to virtual-photon exchange.

The across-horizon effect from electron-muon Coulomb scattering happens due to a non-local correlation between the electron and the muon. This correlation is described by the Feynman propagator. The across-horizon effect resembles, in fact, the state evolution with time of two causally disconnected localized detectors in Minkowski spacetime interacting with each other through a local relativistic quantum field, where the emerging entanglement has been calculated for a simple interaction model by Reznik *et al.* [4]. The extraction of

nonclassical correlations from the quantum vacuum to particle detectors has been called “entanglement harvesting” in the modern literature (cf. Ref. [5] and references therein).

Let us elaborate on the analogy between our across-horizon scattering (Fig. 2) and the setup of Reznik *et al.*, which has two spatially separated detectors in Minkowski spacetime interacting via a relativistic scalar field (see Fig. 1 of Ref. [4]). The muon inside the black-hole horizon and the electron outside can be considered as a pair of causally disconnected “detectors.” The local interaction between our “detectors,” i.e., the muon and the electron, is mediated by the photon field and essentially lasts for a finite time interval of order $\alpha\hbar/E_{\text{CM}}$. As a consequence of the virtual-photon exchange between parts of this relativistic quantum system, the initial state $|\mu, p; e, k\rangle$ evolves unitarily with time and has a finite overlap with a particular final state $|\mu, p'; e, k'\rangle$. The analogy is, of course, not perfect. For example, our “detectors” possess infinitely many energy levels, whereas the setup of Ref. [4] considered two-energy-level detectors (more realistic systems have been considered in, e.g., Ref. [5]).

Returning to our discussion of Coulomb scattering across the Schwarzschild black-hole horizon, the momentum exchange q between inside-particles and outside-particles is a measurable observable (Sec. II and App. C). An outside-observer can measure, in principle, the corresponding momentum change of the outside-particle, but not the charge of the inside-particle or its initial momentum. It appears that the across-horizon-Coulomb-scattering effect can be employed to encode a message, which can be sent by an inside-observer to an outside-observer (Sec. III).

It is sometimes said that “an event horizon is the boundary in spacetime between events that can communicate with distant observers and events that cannot” (quote from Ref. [14], Sec. 11.3). In view of the results of the present article, this statement needs to be refined (the spacetime manifold remains a classical concept): “an event horizon is the boundary in spacetime between events that can communicate with distant observers by classical means and events that cannot.” Nature is, of course, not classical ($\hbar \neq 0$) and this fact allows for a potential breach of the event horizon as defined by the second statement. We have indeed shown that quantum scattering allows, in principle, for the transfer of information from inside the black-hole event horizon to outside.

In this article, we have focussed on across-horizon Coulomb scattering for astrophysical black holes, but similar effects may occur in analogue systems [15, 16].

Appendix A: Initial-particle trajectories

In this appendix, we give an example of initial-particle trajectories which have their closest approach near the Schwarzschild black-hole horizon, with one particle (muon) inside the horizon and the other particle (electron) outside the horizon. Both particles are considered to be ultrarelativistic and c is set to unity. But, before we discuss these initial-particle trajectories, we have a remark on the meaning of the black-hole event horizon.

Generally speaking, the event horizon is a global notion in the sense that it depends on the observer’s entire geodesic history and the large-scale structure of spacetime [12]. The black-hole event horizon, in particular, is associated with a null hypersurface which corresponds to the boundary between null rays that cannot come out and those that can. This horizon surface can be projected locally on the local inertial coordinate system (LICS) of the near-horizon region. By the Einstein Equivalence Principle, the physics in the freely-

falling LICS is the same as that of flat Minkowski spacetime and nothing distinguishes locally the projected horizon surface, only that part of this surface coincides with part of the light-cone.

With appropriate local inertial coordinates $\{T, X, Y, Z\}$ near the Schwarzschild horizon (Fig. 2) and a very large black-hole mass M , the horizon coincides with a disk-like patch of the (Y, Z) -plane centered around $(Y, Z) = (0, 0)$ and at position

$$X_{\text{hor}} = T. \quad (\text{A1})$$

For the initial wave packages, we can take the following trajectories:

$$(X, Y, Z)_{e, \text{in}} \sim \left(-\sqrt{1/3} T + d_0 - d_\mu, \sqrt{2/3} T, 0 \right), \quad (\text{A2a})$$

$$(X, Y, Z)_{\mu, \text{in}} \sim (T - d_\mu, 0, 0), \quad (\text{A2b})$$

where the nonzero particle masses have been neglected for the velocities. The distance between the two wave packages is given by

$$d(T) = \sqrt{(X_\mu - X_e)^2 + (Y_\mu - Y_e)^2 + (Z_\mu - Z_e)^2}, \quad (\text{A3})$$

and the trajectories (A2) result in having $d(0) = d_0$.

An example of these trajectories is given by Fig. 4 [using], where, at the moment of closest approach ($T = 1$), the electron is still outside the horizon, $X_{e, \text{in}}(1) > X_{\text{hor}}(1)$, while the muon is always inside, $X_{\mu, \text{in}}(T) < X_{\text{hor}}(T)$. Dispersion and scattering effects are neglected. The particular initial-particle trajectories of Fig. 4 for a length scale of the order of (4) give the momentum k of the electron and the momentum p of the muon, where k and p enter the amplitude (1).

Remark that, if the muon initially has a velocity with nonzero Y and Z components, the horizon at position (A1) runs away from that particle and the situation sketched in the middle panel of Fig. 4 does not occur. The coordinate X lies, to leading order, in the radial direction of the black-hole spacetime (Fig. 2). The conclusion is, thus, that the initial ultrarelativistic muon (momentum p in Fig. 3) must have, to high precision, an outward radial motion.

Appendix B: Final-particle trajectories

In this appendix, we give a simplified discussion of how Coulomb scattering may affect the motion of the initial particles. In App. C, we give a detailed calculation of the quantum scattering process in position space.

For the initial trajectories of App. A, the large-angle electron-muon Coulomb scattering probability is significant if the minimal distance in Fig. 4 is of order $\alpha \hbar c / E_{\text{CM}}$, based on the estimate (4) in terms of the center-of-mass scattering energy E_{CM} . In that case, there is a nonvanishing probability that the electron recoils. An example of such a recoil trajectory is as follows:

$$(X, Y, Z)_{e, \text{out}} \Big|^{(T>1)} \sim (X_{e, \text{out}, 1} + \sqrt{1/2} (T - 1), Y_{e, \text{out}, 1} + \sqrt{1/2} (T - 1), 0), \quad (\text{B1})$$

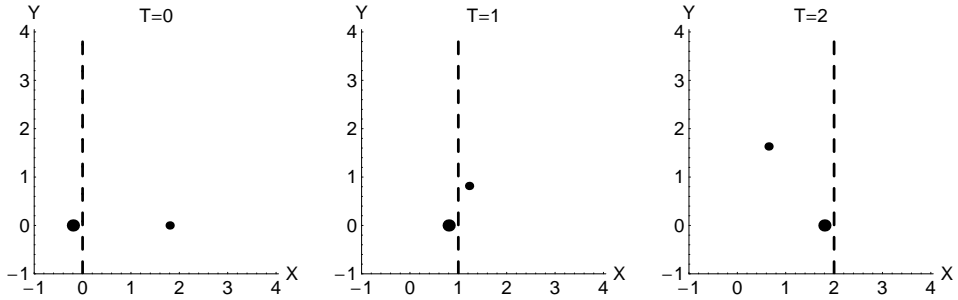


FIG. 4. Initial wave-package trajectories in the (X, Y) -plane from (A2a) and (A2b), without dispersion and scattering. The muon wave package (large dot) has increasing values of X and a constant value of Y . The electron wave package (small dot) has decreasing values of X and increasing values of Y . The projected black-hole horizon from (A1) is shown as the dashed line. With an arbitrary length unit, the parameters in (A2) are chosen as $\{d_0, d_\mu\} = \{2, 1/5\}$. The minimum separation $d_{\min} \approx 0.92$ occurs at $T_{\min} = 1$. For a length scale of the order of (4), significant Coulomb scattering occurs, as discussed in Sec. III and App. C.

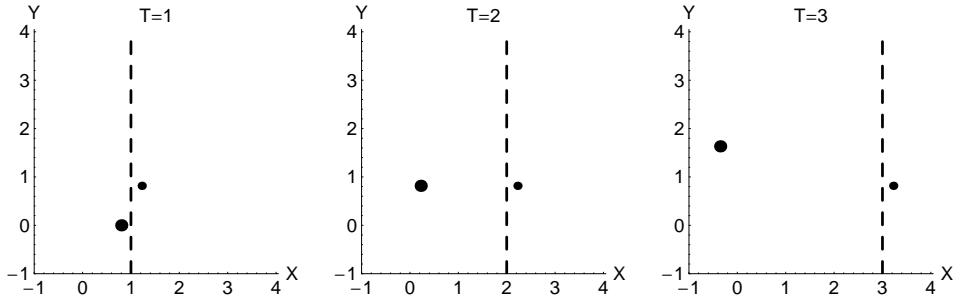


FIG. 5. Final wave-package trajectories in the (X, Y) -plane from (B2a) and (B2b), with Coulomb scattering taking place at $T \sim 1$. The constants $(X_{e,\text{out},1}, Y_{e,\text{out},1})$ and $(X_{\mu,\text{out},1}, Y_{\mu,\text{out},1})$ have been taken equal to the $T = 1$ positions of the initial-particle trajectories (A2a) and (A2b), as shown in Fig. 4 for $T \leq 1$ and a length scale of the order of (4).

with a matching muon trajectory from energy-momentum conservation and a length unit equal to (4). The constants $(X_{e,\text{out},1}, Y_{e,\text{out},1})$ in (B1) correspond approximately to the position of the initial electron at $T = 1$ in Fig. 4. A recoil electron with trajectory (B1) is, however, rapidly overrun by the horizon at position (A1). Remark that, for a genuine scattering process, we should only consider the electron in (B1) at $T \gg 1$, but we have simplified the discussion somewhat by taking $T > 1$.

Consider, next, a different trajectory of the recoil electron,

$$(X, Y, Z)_{e,\text{out}} \Big|^{(T>1)} \sim (X_{e,\text{out},1} + (T-1), Y_{e,\text{out},1}, 0), \quad (\text{B2a})$$

$$(X, Y, Z)_{\mu,\text{out}} \Big|^{(T>1)} \sim (X_{\mu,\text{out},1} - \sqrt{1/3}(T-1), Y_{\mu,\text{out},1} + \sqrt{2/3}(T-1), 0), \quad (\text{B2b})$$

with constants $(X_{e,\text{out},1}, Y_{e,\text{out},1})$ and $(X_{\mu,\text{out},1}, Y_{\mu,\text{out},1})$ corresponding approximately to

the positions of the initial particles at $T = 1$ in Fig. 4. Now, the final electron has a velocity purely in the X direction and the final electron stays outside the horizon, provided $X_{e,\text{out},1} > 1$. Figure 5 shows these final trajectories, again using (4) as the length unit. The particular final-particle trajectories of Fig. 5 for a length scale of the order of (4) give the momentum k' of the electron and the momentum p' of the muon, where k' and p' enter the amplitude (1).

The final recoil electron of (B2a) is special in that its Y and Z velocity components are exactly zero. Let us estimate which changes in that velocity direction are allowed if we demand that the final ultrarelativistic recoil electron stays outside the black-hole horizon, at least, over the Minkowski patch considered.

The curvature scale is given by $r_S = 2G_N M/c^2 \approx 3 \text{ km}$ (M/M_{Sun}) and the Minkowski patch has approximately that size. If we now assume that, just after the scattering moment $T \sim 1$, the recoil electron is outside the horizon by a distance $\tilde{d} \sim X_{e,\text{out},1} - 1 \sim \alpha \hbar c/E_{\text{CM}} \approx 1.4 \times 10^{-18} \text{ m}$ (GeV/E_{CM}) in the X direction, then we find that the electron trajectory can differ from the trajectory (B2a) by a small angle δ which is of order

$$\delta \sim \sqrt{2 \tilde{d}/r_S} \sim \sqrt{\alpha} E_P / \sqrt{E_{\text{CM}} M c^2}, \quad (\text{B3})$$

with Planck energy $E_P \equiv \sqrt{\hbar c^5/G_N} \approx 1.22 \times 10^{19} \text{ GeV} \approx 2.18 \times 10^{-5} \text{ g}$. Hence, the allowed solid angle δ^2 of the recoil electron (momentum k' in Fig. 3) is extremely small: $\delta^2 \sim 10^{-36}$ for $E_{\text{CM}} \sim 10^{15} \text{ GeV}$ and $M \sim M_{\text{Sun}} \sim 10^{38} E_P$.

A related issue is that the recoil electron must have a sufficiently large energy [a large enough gamma factor $E(k')/(m_e c^2)$], so that the electron is not overrun by the horizon (A1) before the electron reaches the edge of the Minkowski patch at $X \sim r_S$. Taking that the recoil electron at $T \sim 1$ is outside the horizon by a distance $\tilde{d} \sim \alpha \hbar c/E_{\text{CM}}$ in the X direction, and assuming a velocity purely in the X direction and an energy of order $E_{\text{CM}}/2$, we get the following estimate for the required center-of-mass scattering energy:

$$E_{\text{CM}} \gtrsim 4 \frac{1}{\alpha} \frac{m_e c^2}{E_P} \frac{M c^2}{E_P} m_e c^2, \quad (\text{B4})$$

where $m_e \approx 0.511 \text{ MeV}/c^2$ is the electron mass and M the black-hole mass. With $M \sim M_{\text{Sun}}$, the required scattering energy is $E_{\text{CM}} \gtrsim 10^{15} \text{ GeV}$, which is large but still less than the Planck energy E_P .

Considering the curved spacetime manifold of the Schwarzschild black hole, it can be verified that (B4) corresponds to the condition for radial escape of the recoil electron if its initial energy is of order E_{CM} in the relevant local inertial frame near the horizon and its initial position is at a proper distance (4) outside the horizon. As the recoil electron escapes towards infinity (point i^+ of Fig. 3), its energy is red-shifted; cf. Sec. 25.4 in Ref. [13].

The conclusion is that both estimates (B3) and (B4) prefer a relatively small value of the black-hole mass M . Practical considerations, on the other hand, may favor a relatively large value of M , as discussed in the point 4a and the last paragraph of Sec. III.

Appendix C: Scattering probability amplitude in position space

In this appendix, we discuss the elastic scattering process (1) in position space. Here, we will directly follow Feynman's seminal paper [6]. An alternative calculation with auxiliary

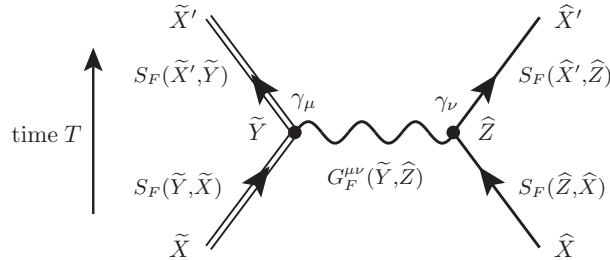


FIG. 6. Position-space Feynman diagram for elastic electron-muon scattering (adapted from Fig. 1 of Ref. [6]). The external muon is denoted by a double line and the external electron by a single line, where the flow of negative electric charge is indicated by an arrow. The Feynman propagator of the photon is denoted by a wavy line. The spacetime positions of the two interaction vertices (dots) are to be integrated over. The corresponding probability amplitude is given by (C1).

momentum variables has been presented in App. C of an earlier version of the present article [17]. Throughout this appendix, we use the Cartesian coordinates $(X)^\mu = (T, X, Y, Z)^\mu$ with Minkowski metric $\eta_{\mu\nu}$. These coordinates appeared as local inertial coordinates in Fig. 2 and were already used in Apps. A and B.

We start from the original Feynman amplitude for 2-2 scattering in position space, which is given by Eq. (4) in Ref. [6]. Making some minor changes in notation (cf. Fig. 6), we have the following tree-level probability amplitude for an electron to propagate from \hat{X} to \hat{X}' and a muon from \tilde{X} to \tilde{X}' :

$$A(\tilde{X}'; \hat{X}' | \tilde{X}; \hat{X}) \Big|_{\text{tree}} = -e^2 \int d^4 \tilde{Y} d^4 \hat{Z} \times S_F(\tilde{X}', \tilde{Y}) \gamma_\mu S_F(\tilde{Y}, \tilde{X}) G_F^{\mu\nu}(\tilde{Y}, \hat{Z}) S_F(\hat{X}', \hat{Z}) \gamma_\nu S_F(\hat{Z}, \hat{X}), \quad (\text{C1})$$

where S_F corresponds to the Feynman propagator of the fermionic field (spinor indices are suppressed everywhere) and $G_F^{\mu\nu}$ is the Feynman propagator of the photon field in the Feynman gauge,

$$G_F^{\mu\nu}(X', X) = -\frac{1}{4\pi^2} \frac{\eta^{\mu\nu}}{[X' - X]^2 - i\epsilon}, \quad (\text{C2})$$

with the shorthand notation $[X' - X]^2 \equiv (X'^\rho - X^\rho)(X'_\rho - X_\rho)$. The Feynman propagator $G_F^{\mu\nu}(X', X)$ is also nonvanishing for spacelike separated points X' and X . In the contrast, the retarded Green's function of the photon field (relevant to classical processes) only has a nonvanishing support for light-like separated points X' and X ,

$$G_R^{\mu\nu}(X', X) = \frac{i}{2\pi} \eta^{\mu\nu} \theta(X'^0 - X^0) \delta([X' - X]^2). \quad (\text{C3})$$

Now take the following $\{T, X, Y, Z\}$ values for the spacetime positions of the initial and

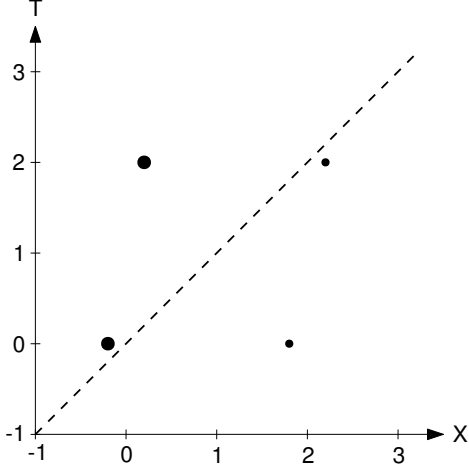


FIG. 7. Spacetime diagram with the positions (C4) of the initial and final particles for the electron-muon scattering process considered (Fig. 6), where the large dot corresponds to the muon μ^- and the small dot to the electron e^- . Only the T and X coordinates are shown. The initial positions at $T = 0$ correspond to the colliding wave packages of Fig. 4 and the final positions at $T = 2$ correspond to the separating wave packages of Fig. 5. The dashed curve corresponds to a slice of the projected black-hole horizon, $\{X, Y, Z\}_{\text{horizon}} \text{ at time } T = \{T, Y, Z\}$.

final particles:

$$\hat{X}_{\text{electron}} = \left\{ 0, +9/5, 0, 0 \right\}, \quad (\text{C4a})$$

$$\tilde{X}_{\text{muon}} = \left\{ 0, -1/5, 0, 0 \right\}, \quad (\text{C4b})$$

$$\hat{X}'_{\text{electron}} = \left\{ 2, 14/5 - \sqrt{1/3}, \sqrt{2/3}, 0 \right\}, \quad (\text{C4c})$$

$$\tilde{X}'_{\text{muon}} = \left\{ 2, 4/5 - \sqrt{1/3}, \sqrt{2/3}, 0 \right\}, \quad (\text{C4d})$$

where, for definiteness, we have used the values from Figs. 4 and 5 for a length scale of the order of (4). The positions (C4) are shown in Fig. 7, together with the projected black-hole horizon (dashed curve) as discussed in Fig. 2 and App. A. The leading-order probability amplitude for the electron-muon scattering considered in Figs. 6 and 7 is then given by the scalar product of the initial and final wave packages of the particles with the tree-level amplitude (C1).

Specializing to the initial and final positions of Fig. 7, the tree-level amplitude (C1) is nonzero, as the Feynman propagator G_F also has support outside the lightcone and is nonzero even for spacelike separations. The corresponding probability is then nonvanishing and gives the recoil electron needed for the *Gedankenexperiment* of Sec. III.

Let us end this appendix by discussing the elastic electron-muon scattering process (Fig. 6) in Minkowski spacetime *per se*, leaving aside the application to black holes. In order to simplify the discussion, we temporarily restrict to 1 + 1 spacetime dimensions (coordinates T and X). We take it that the colliding particles have positions at $T = 0$ as given by Fig. 7 and that a recoil electron at $T = 2$ is detected at the position shown by Fig. 7.

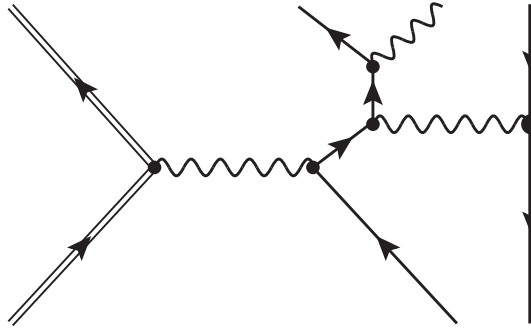


FIG. 8. Position-space Feynman diagram for electron-muon scattering (Fig. 6) with Bremsstrahlung from the scattered electron as it is deflected by a nucleus (symbolically shown by the heavy line on the right). For the Bremsstrahlung of the scattered electron, there are, in general, two more Feynman diagrams to consider; cf. Fig. 6-21 of Ref. [7]. The spacetime positions of the five interaction vertices (dots) are to be integrated over.

Specifically, there is then a right-moving recoil electron detected *outside* the right-moving lightcone of the initial muon at $T = 0$. Observe that the process does not involve faster-than- c propagation of light [18], which, incidentally, may still be consistent with causality [19, 20]. Rather, there is the propagation of a *virtual* photon over a *spacelike* distance, as discussed in Sec. I.

Note that, due to the nonzero mass of the electron, the right-moving recoil electron of Fig. 7 will ultimately get *inside* the right-moving lightcone of the initial muon. As mentioned already in App. B, we should, for a genuine scattering process, only consider final particles at $T \gg 2$ and initial particles at $T \ll 0$. For this genuine scattering process, the time-ordering of the initial and final particles is invariant under the action of proper orthochronous Lorentz transformations.

Now consider the following modification of this elastic scattering process: a subprocess is added which transfers the information from the “detection” of a right-moving electron at $T = 2$ in Fig. 7 to a right-moving electromagnetic signal. This right-moving electromagnetic signal does stay outside the right-moving lightcone of the initial muon. At the microscopic level, the subprocess can be realized as Bremsstrahlung [7] from the scattered electron as it is deflected by a nucleus; see Fig. 8. There is, then, a small but nonvanishing probability to get a right-moving hard photon which stays outside the right-moving lightcone of the initial muon. (Causality holds as long as the right-moving hard photon is inside the right-moving lightcone of the initial electron or nucleus; see also the discussion below Eq. (3.8) and Fig. 3 in Ref. [21].) It will be a challenge to design a Minkowski-spacetime experiment to demonstrate this QED effect with a final hard photon outside the lightcone of the initial muon.

[1] S.W. Hawking, “Particle creation by black holes,” *Commun. Math. Phys.* **43**, 199 (1975), Erratum: *Commun. Math. Phys.* **46**, 206 (1976).

[2] W.G. Unruh and R.M. Wald, “Information loss,” *Rept. Prog. Phys.* **80**, 092002 (2017), arXiv:1703.02140.

[3] V.A. Emelyanov, “QED loop effects in the spacetime background of a Schwarzschild black hole,” *J. Phys. Conf. Ser.* **942**, 012009 (2017), arXiv:1710.01049.

[4] B. Reznik, A. Retzker, and J. Silman, “Violating Bell’s inequalities in the vacuum,” *Phys. Rev. A* **71**, 042104 (2005), arXiv:quant-ph/0310058.

[5] A. Pozas-Kerstjens and E. Martin-Martinez, “Entanglement harvesting from the electromagnetic vacuum with hydrogenlike atoms,” *Phys. Rev. D* **94**, 064074 (2016), arXiv:1605.07180.

[6] R.P. Feynman, “Space-time approach to quantum electrodynamics,” *Phys. Rev.* **76**, 769 (1949).

[7] C. Itzykson and J.B. Zuber, *Quantum Field Theory* (McGraw-Hill, New York, USA, 1980).

[8] M.J.G. Veltman, *Diagrammatica: The Path to Feynman Rules* (Cambridge University Press, England, 1994).

[9] M.E. Peskin and D.V. Schroeder, *An Introduction to Quantum Field Theory* (Addison-Wesley Publishing Co., 1995).

[10] M.D. Schwartz, *Quantum Field Theory and the Standard Model* (Cambridge University Press, England, 2014).

[11] R. Gautreau, “Light cones inside the Schwarzschild radius,” *Am. J. Phys.* **63**, 431 (1995).

[12] S.W. Hawking and G.F.R. Ellis, *The Large Scale Structure of Space-Time* (Cambridge University Press, England, 1973).

[13] C.W. Misner, K.S. Thorne, and J.A. Wheeler, *Gravitation* (W.H. Freeman and Co., San Francisco, 1973).

[14] B.F. Schutz, *A First Course in General Relativity*, Second Edition (Cambridge University Press, England, 2009).

[15] S. Weinfurtner, E.W. Tedford, M.C.J. Penrice, W.G. Unruh, and G.A. Lawrence, “Measurement of stimulated Hawking emission in an analogue system,” *Phys. Rev. Lett.* **106**, 021302 (2011), arXiv:1008.1911.

[16] L.-P. Euvé, F. Michel, R. Parentani, T.G. Philbin, and G. Rousseaux, “Observation of noise correlated by the Hawking effect in a water tank,” *Phys. Rev. Lett.* **117**, 121301 (2016), arXiv:1511.08145.

[17] V.A. Emelyanov and F.R. Klinkhamer, “Across-horizon scattering and information transfer,” arXiv:1710.06405v6.

[18] I.T. Drummond and S.J. Hathrell, “QED vacuum polarization in a background gravitational field and its effect on the velocity of photons,” *Phys. Rev. D* **22**, 343 (1980).

[19] S. Liberati, S. Sonego, and M. Visser, “Faster-than- c signals, special relativity, and causality,” *Annals Phys.* **298**, 167 (2002), arXiv:gr-qc/0107091.

[20] F.R. Klinkhamer and M. Schreck, “Consistency of isotropic modified Maxwell theory: Micro-causality and unitarity,” *Nucl. Phys. B* **848**, 90 (2011), arXiv:1011.4258.

[21] R. Dickinson, J. Forshaw, P. Millington, and B. Cox, “Manifest causality in quantum field theory with sources and detectors,” *JHEP* **1406**, 049 (2014), arXiv:1312.3871.